SIAM J. Applied Dynamical Systems
Vol. xx, pp. x

Coherent structures in a population model for mussel-algae interaction.

Anna Ghazaryan[†] and Vahagn Manukian[‡]

Abstract. We consider a known model that describes formation of mussel beds on soft sediments. The model consists of nonlinearly coupled pdes that capture evolution of mussel biomass on the sediment and algae in the water layer overlying the mussel bed. The system accounts for the diffusive spread of mussels, while the diffusion of algae is neglected and at the same time the tidal flow of the water is considered to be the main source of transport for algae, but does not affect mussels. Therefore, both the diffusion and the advection matrices in the system are singular. A numerical investigation of this system in some parameter regimes is known. We present a systematic analytic treatment of this model. Among other techniques we use Geometric Singular Perturbation Theory to analyze the nonlinear mechanisms of pattern and wave formation in this system.

1. Introduction.

The ability of mussels to self-organize has been known to the ecologists (see [14] and references within). In recent years, a significant interest towards using mathematics to understand the mechanisms of the phenomenon of aggregation and pattern formation in mussel beds has been noticeable. Predator-prey models have been suggested to explain pattern formation in mussel beds. Some of them are restricted to mussel and algae interactions [14, 15], some, in addition, include a description of sediment accumulation [11].

In an important work [10] the role of the phase separation in pattern formation on mussel beds was pointed out. Cahn-Hilliard equation was demonstrated to successfully describe patterns observable in field experiments. In [10] density-dependent movement as opposed to scale-dependent activator-inhibitor feedback is recognized the first time as a general mechanism of pattern formation in ecology. The dynamics illustrated by Cahn-Hilliard equation captures interpolation between two stable phases that happens on short-time scales rather than the intermediate or long-range dynamics induced by an instability of a phase.

Current work is concentrated on the two-component partly parabolic system of partial differential equations related to the system introduced in [14] which we describe below. The scaling that we use in this system is effective for longer time scales compared to the ones studied in [10]. On such time scales as it is mentioned in [10] the mortality and individual growth of mussels dominate the shape of the mussel bed.

Van de Koppel and collaborators in [14] introduced the following system as a model for prey-predator interaction between algae and mussels with a linear functional response,

$$\begin{aligned} A_\tau &= (A_{up} - A)f - \frac{c}{h}AM - \nu A_x, \\ M_\tau &= ecAM - d_M \frac{k_m}{k_m + M}M + D(M_{xx} + M_{yy}). \end{aligned} \tag{1.1}$$

Here $A = A(x, y, \tau)$ is the concentration of algae in the water layer and $M = M(x, y, \tau)$ is the mussel biomass per square meter of sediment surface, (x, y) is the two-dimensional space

[†]Miami University, Oxford, Ohio, USA (ghazarar@miamioh.edu). Supported by the NSF grant DMS-1311313.

[‡]Miami University, Hamilton, Ohio, USA (manukive@miamioh.edu). Supported by the grant #246535 from the Simons Foundation.

that represents sediment surface, and τ is the time. All of the constants in this model are non-negative. A_{up} is the concentration of algae in the upper water level, f is the rate of exchange between the lower and upper levels, c is the consumption constant, h is the height of the lower water level, e is the conversion constant of ingested algae to mussel production, and ν characterizes the rate at which algae is supplied to the mussel bed by the water flow. This rate is assumed in [14] to be constant since the algae is supplied to the mussel bed mainly via the flood flow.

The mussel mortality is assumed to decrease when mussel density increases because of a reduction of dislodgment and predation in dense clumps. This assumption is represented in the term $k_m/(k_m+M)$, where k_M is the value of M at which mortality is half of the maximal. Constant D is the diffusion rate of the mussels. The diffusion rate of mussels depends on their age. Mussels in young beds diffuse at faster rates than in the mature beds. We refer the reader to [14] for detailed explanation of the deduction of the model and references on which it is based, as well as the tables of representative values of the parameters.

In this paper we will consider a one-dimensional version of (1.1),

$$\begin{aligned} A_\tau &= (A_{up}-A)f - \frac{c}{h}AM - \nu A_x, \\ M_\tau &= ecAM - d_M\frac{k_m}{k_m+M}M + DM_{xx}. \end{aligned} \tag{1.2}$$

To find traveling waves, we assume that the model is posed on unbounded space $(x,\tau)\in\mathbb{R}\times\mathbb{R}^+$ to allow for propagation of the mussels. This is valid when the coupling of diffusion to the reaction kinetics is weak or the internal length of the system is much smaller than the size of the domain (the size of a mussel compared to the size of the sea shore). According to Fife [8], the boundary effects do not play too much role in the pattern forming mechanism in the interior of the domain and traveling waves considered on an infinite domain reveal physically relevant phenomena.

It is known that even for young mussels the values of parameter D are quite small compared to the values of other parameters (about 10^{-3} times smaller, see Table 1 in [14]) so we think of D as a small parameter no matter whether mussel beds are young or mature.

In [14], van de Koppel and collaborators performed numerical simulations on a non - dimensionalized version of the system (1.2), which reads

$$\begin{aligned} a_t &= \tilde{\alpha}(1-a) - am - \tilde{\beta}a_x, \\ m_t &= \tilde{\delta}am - \tilde{\gamma}\frac{m}{1+m} + m_{xx}, \end{aligned} \tag{1.3}$$

where the relationships between the new and the original quantities are

$$a = A_{up}^{-1}A, \quad m = k_M^{-1}M, \quad T = ck_Mh^{-1},$$

the space and time are scaled as $x = T^{1/2}D^{-1/2}X$, and $t = T\tau$, and new parameters are

$$\tilde{\alpha} = fT^{-1}, \quad \tilde{\beta} = VD^{-1/2}T^{-1/2}, \quad \tilde{\gamma} = d_MT^{-1}, \quad \tilde{\delta} = ecA_{up}T^{-1}.$$

The study in [14] is focused on the relation of pattern formation on the mussel bed with the resilience of mussel bed systems to disturbances. Among other things, the authors demonstrated that self-organized spatial patterns improve the resilience of mussel beds. We refer readers to the original paper for detailed ecological implications of the results obtained in [14]. In a follow-up paper [15] further investigation of periodic patterns in the same system was performed numerically using AUTO [4]. The authors also briefly mentioned in Section 4 that for certain parameter values monotone or oscillatory traveling waves in the system have been observed in AUTO calculations.

In this paper we present a systematic analytical study of traveling waves in (1.2). We consider a non-dimensionalization of (1.2) that is different from (1.3), as it represents a different time and space scalings as well as a different scaling for M. More precisely, we keep the spatial variable the same as in (1.2) and set $t = ecA_{up}\tau$, then denote $u(x,t) = A(x,t)/A_{up} = a(x,t)$ and $v(x,t) = fhc^{-1}M(x,t)$. The system (1.2) then reads

$$\begin{aligned} u_t &= \frac{f}{ec}(1-u-uv) - \frac{\nu}{ecA_{up}}u_x, \\ v_t &= uv - \frac{d_m}{ecA_{up}}\frac{v}{(1+fh(ck_m)^{-1}v)} + \frac{D}{ecA_{up}}v_{xx}. \end{aligned} \tag{1.4}$$

Using the following notations

$$\delta = f(ec)^{-1},\ \ \alpha = fh(ck_m)^{-1},\ \ \varepsilon = D(A_{up}ec)^{-1},\ \ \beta = \nu(ecA_{up})^{-1},\ \ \gamma = d_m(ecA_{up})^{-1}, \tag{1.5}$$

we then rewrite the system (1.4) as

$$\begin{aligned} u_t &= \delta(1-u-uv) - \beta u_x, \\ v_t &= uv - \gamma\frac{v}{1+\alpha v} + \varepsilon v_{xx}. \end{aligned} \tag{1.6}$$

This system has one more parameter than the system (1.3), but we prefer to keep ε in the system and not scale it out because it is related to D which as we mentioned above is much smaller than the rest of the parameters in the system and thus will be treated as a small parameter in our analysis which is based on the Singular Perturbation Theory.

An alternative approach is to scale out β from the first equation, thus moving it into the new diffusion coefficient ε/β^2, but since we are interested in traveling waves, we aim to simplify the system (1.6) after we rewrite it in the moving coordinates, in the next section, because introducing a moving frame generates additional convection terms. In the next section we demonstrate that this scaling produces a form which is convenient for bifurcation analysis of traveling waves.

Traveling waves are solutions of the underlying partial differential equation that preserve their shape while propagating to an infinity. They are important solutions that sometimes arise in partial differential equations posed on infinite domains. If stable, these solutions are observed as coherent structures in the system. If unstable, the type of their instability dictates how solutions that start near the traveling waves behave. There are different types of traveling waves, but in this work we are interested in periodic wave trains, traveling waves that asymptotically connect two different constant states, and traveling waves that connect

a periodic wave train to a constant state. The former are called fronts, and the latter can be considered a generalization of the fronts. Schematically, these waves are represented in Figure 1.1.

Figure 1.1. *The existence of the following types of waves is shown in this work: a) fronts with monotone tails and fronts with oscillatory tails, b) fronts that connect a periodic wave train to a spatially homogeneous state, c) periodic wave trains.*

2. Existence of traveling waves.

We are interested in traveling wave solutions of the coupled system of partial differential equations (1.4). To analyze the existence of traveling waves, we consider system (1.4) in a moving coordinate frame $\xi = x - ct$, where c is a parameter that represents the speed of the wave. System (1.4) in the new coordinate frame reads

$$\begin{aligned} u_t &= \delta(1-u-uv) + (c-\beta)u_\xi, \\ v_t &= uv - \frac{\gamma v}{1+\alpha v} + cv_\xi + \varepsilon v_{\xi\xi}. \end{aligned} \tag{2.1}$$

Traveling waves are stationary solutions of this system of partial differential equations. As such, they can be sought as solutions of the following system of ordinary differential equations,

$$\begin{aligned} (c-\beta)u_\xi + \delta(1-u-uv) &= 0, \\ \varepsilon v_{\xi\xi} + cv_\xi + uv - \frac{\gamma v}{1+\alpha v} &= 0. \end{aligned} \tag{2.2}$$

We note that here different signs of c may lead to solutions of qualitatively different types. We rescale the spatial variable ξ in the system (2.2) as $\xi = cz$, and introduce our bifurcation parameter η and a new parameter ϵ as

$$\eta = \frac{c\delta}{c-\beta}, \qquad \epsilon = \frac{\varepsilon}{c^2}. \tag{2.3}$$

The parameter η is a technical parameter. It is related to δ and, obviously, captures the direction of propagation of the front relative to the current, but mainly it controls the relative

strength of the reaction terms in the traveling wave equations (2.2) which then become

$$\begin{aligned} u' + \eta(1 - u - uv) &= 0, \\ \epsilon v'' + v' + uv - \frac{\gamma v}{1 + \alpha v} &= 0, \end{aligned} \tag{2.4}$$

where the derivative is taken with respect to z. This system can be written as a first order system for $u_1 = u$, $v_1 = v$, and $v_2 = v'$,

$$\begin{aligned} u_1' &= \eta(u_1 v_1 + u_1 - 1), \\ v_1' &= v_2, \\ \epsilon v_2' &= -v_2 + \frac{\gamma v_1}{1 + \alpha v_1} - u_1 v_1, \end{aligned} \tag{2.5}$$

or, equivalently, in a coordinate $\zeta = z/\epsilon$,

$$\begin{aligned} \dot{u}_1 &= \epsilon\eta(u_1 v_1 + u_1 - 1), \\ \dot{v}_1 &= \epsilon v_2, \\ \dot{v}_2 &= -v_2 + \frac{\gamma v_1}{1 + \alpha v_1} - u_1 v_1, \end{aligned} \tag{2.6}$$

where the derivative is taken with respect to ζ. We shall refer to system (2.5) as the slow system and (2.6) as the fast system. These two systems are equivalent when $\epsilon \neq 0$. They have the same equilibria. The point $A = (1, 0, 0)$ is an equilibrium regardless the values of α and γ. When $\gamma = \alpha = 1$, there is a curve of equilibrium points $\Gamma_1 = \{(1/(1 + v_1), v_1, 0)\}$ that contains A. When $\gamma = 1$ but $\alpha \neq 1$ and when $\gamma \neq 1$ but $\alpha = \gamma$ the only equilibrium is at A. In the complement to the union of the lines $\gamma = 1$ and $\gamma = \alpha$ there are exactly two distinct equilibria

$$A = (1, 0, 0) \text{ and } B = \left(\frac{\alpha - \gamma}{\alpha - 1}, \frac{\gamma - 1}{\alpha - \gamma}, 0\right).$$

Due to the physical meaning of the quantities involved, we are interested in parameter regimes that yield nonnegative coordinates of B, and, moreover, in connections between equilibria A and B with always nonnegative u_1 and v_1- components. Therefore, within the complement to $\{\gamma = 1 \cup \gamma = \alpha\}$ in the (γ, α)-plane, we only consider sectors

$$1 < \gamma < \alpha \text{ and } 0 < \alpha < \gamma < 1. \tag{2.7}$$

The equilibrium points A and B (when α and γ are as in (2.7)) are schematically represented in Figure 2.1 on $(u_1, v_1, 0)$-plane. The equilibrium A is the intersection of the curve $\Gamma_1 = \{(1/(1 + v_1), v_1, 0)\}$ with the curve $\Gamma_2 = \{(u_1, 0, 0)\}$ and the equilibrium B is the intersection of the curve Γ_1 with the curve $\Gamma_3 = \{(\gamma/(1 + \alpha v_1), v_1, 0)\}$. The point $C = (\gamma, 0, 0)$ is not an equilibrium, but will be used to describe phenomenologically different cases.

When $\epsilon = 0$, a reduced system can be obtained from (2.5) as follows. The last equation in (2.5) reduces to

$$-v_2 + \frac{\gamma v_1}{1 + \alpha v_1} - u_1 v_1 = 0.$$

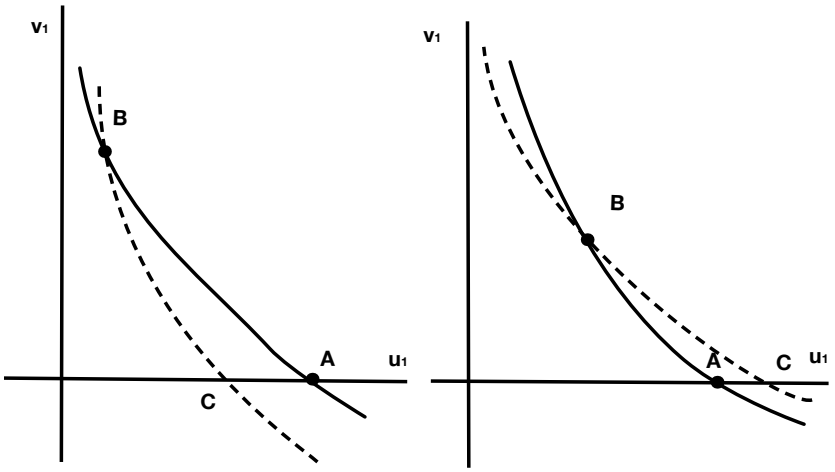

Figure 2.1. *Nullclines and equilibria on* $(u_1, v_1, 0)$*-plane:* $A = (1, 0, 0)$ *and* $B = (\frac{\alpha-\gamma}{\alpha-1}, \frac{\gamma-1}{\alpha-\gamma}, 0)$ *are the equilibrium points.* $C = (\gamma, 0, 0)$ *is an auxiliary point. The dashed curve is* $\Gamma_3 = \{(\gamma/(1+\alpha v_1), v_1, 0)\}$ *and the solid curve is* $\Gamma_1 = \{(1/(1+v_1), v_1, 0)\}$.

On this set, the limiting slow equations are

$$\begin{aligned} u_1' &= \eta(u_1 v_1 + u_1 - 1), \\ v_1' &= \frac{\gamma v_1}{1+\alpha v_1} - u_1 v_1. \end{aligned} \tag{2.8}$$

On the other hand, the system (2.6) in the limit $\epsilon \to 0$ is

$$\begin{aligned} u_1' &= 0, \\ v_1' &= 0, \\ v_2' &= -v_2 + \frac{\gamma v_1}{1+\alpha v_1} - u_1 v_1. \end{aligned} \tag{2.9}$$

The set

$$M(0) = \{(u_1, v_1, v_2) : \ v_2 = \frac{\gamma v_1}{1+\alpha v_1} - u_1 v_1\}$$

is a two-dimensional set of equilibria for (2.9). The linearization of the system (2.9) about any point in this set has two zero eigenvalues and one negative eigenvalue. Therefore $M(0)$ is an invariant, normally hyperbolic, and attracting set for (2.6). Under these conditions invariant manifold theory by Fenichel is applicable. More precisely, by Fenichel's First Theorem ([7], [9, Fenichel's Invariant Manifold Theorem 1]), the critical set $M(0)$, at least over compact sets, perturbs to an invariant set $M(\epsilon)$ for (2.6) with $\epsilon > 0$ but sufficiently small. The distance between $M(0)$ and $M(\epsilon)$ is of order ϵ,

$$M(\epsilon) = \{(u_1, v_1, v_2) : v_2 = \frac{\gamma v_1}{1+\alpha v_1} - u_1 v_1 + \mathrm{O}(\epsilon)\}.$$

If ϵ is small enough, $M(\epsilon)$ is also normally hyperbolic and attracting on the fast scale $\zeta = z/\epsilon$. The slow flow on $M(\epsilon)$ is given by

$$\begin{aligned} \dot{u}_1 &= \epsilon(\eta(v_1 u_1 - 1 + u_1) + \mathrm{O}(\epsilon)), \\ \dot{v}_1 &= \epsilon(\frac{\gamma v_1}{1+\alpha v_1} - u_1 v_1 + \mathrm{O}(\epsilon)). \end{aligned} \tag{2.10}$$

Recall that the reduced flow on the critical manifold is given by (2.8).

In the next few sections we will take a closer look at the flow generated by the reduced system (2.6). The analysis depends on the parameters α, γ and η. Notice that the sign of η is determined by the sign of c and the sign of $c-\beta$, in other words, it is determined by the relation between the speed of the current and the speed of the traveling wave. We find it convenient to divide the three-dimensional parameter space on the following regions:

(i) Region 1: $1 < \gamma < \alpha$, $\eta < 0$;
(ii) Region 2: $0 < \alpha < \gamma < 1$, $\eta < 0$;
(iii) Region 3: $1 < \gamma < \alpha$, $\eta > 0$;
(iv) Region 4: $0 < \alpha < \gamma < 1$, $\eta \in \left(0, \frac{\alpha(\gamma-1)(\alpha-\gamma)^2}{(\alpha-1)^3\gamma}\right)$;
(v) Region 5: $0 < \alpha < \gamma < 1$, $\eta \in \left[\frac{\alpha(\gamma-1)(\alpha-\gamma)^2}{(\alpha-1)^3\gamma}; \infty\right)$.

This division of the parameter space is based on changing character of the equilibria A and B. Indeed, in Region 1, A is a saddle and B is an attractor; in Region 2, B is a saddle and A is a stable node; in Region 3, B is a saddle and A is an unstable node; in Region 4, B is a stable node and A is a saddle.

In this paper we concentrate on Regions 1, 2, 3, and 4.

In Regions 1, 2, and 3 we use "non-traditional" trapping region type argument to prove the existence of the orbits in the reduced system. The argument is based on the fact that for each of these parameter regimes there exists two singular orbits that can serve as boundaries of the trapping region, despite the fact that they do not exists for the same parameters. They are in some sense "invisible" obstacles. We present these arguments in Section 3. Dimension counting then shows that the orbits that exists in the reduced system persist in the full system.

In Region 4 there is no trapping region to use. Instead, in Section 4, to show the existence of a periodic orbit and an orbit that connects the periodic orbit to a constant state, we use the analysis of the vector field using Hopf bifurcation theorem, as well as the compactification technique along with the Poincaré-Bendixson theorem.

Region 5 is not studied in this paper.

3. Existence of heteroclinic orbits.

3.1. Region 1: $1 < \gamma < \alpha$, $\eta < 0$.

Theorem 3.1. *For each fixed α, η, γ from Region 1, there exists $\epsilon_0 = \epsilon_0(\alpha, \eta, \gamma) > 0$ such that for any $\epsilon < \epsilon_0$ there is a heteroclinic orbit that connects a saddle A to a stable node B.*

Remark 3.2. *Existence of a heteroclinic orbit implies that in the system (2.2) with fixed α, γ such that $1 < \gamma < \alpha$, fixed δ, $\beta > 0$, and fixed $0 < c < \beta$ there exists $\tilde{\varepsilon} = \tilde{\varepsilon}(\delta, \beta, c, \gamma, \alpha) > 0$ such that there is a front solution that moves with a speed c for any $\varepsilon < \tilde{\varepsilon}$. Here $\tilde{\varepsilon} = c^2\epsilon_0$, where ϵ_0 is as in Theorem 3.1 and therefore implicitly depends on c. We note that the exact nature*

of the dependence of $\tilde{\varepsilon}$ on c is not revealed by the methods that we used to prove Theorem 3.1.

Remark 3.3. *Here and throughout the paper when we say "a front" we mean a front together with the family of its translates.*

In this particular parameter regime it is guaranteed that, in the plane $v_2 = 0$, the equilibrium $A = (1, 0, 0)$ in Figure 3.1 is strictly to the left of the point $C = (\gamma, 0, 0)$.

We consider the reduced system (2.8). The parameter η in this regime is negative, so we denote $|\eta| = \sigma_1$ and write (2.8) as

$$\begin{aligned} u_1' &= -\sigma_1(v_1 u_1 - 1 + u_1), \\ v_1' &= \frac{\gamma v_1}{1 + \alpha v_1} - u_1 v_1. \end{aligned} \tag{3.1}$$

We will treat this system as a system with a multi-scale structure imposed by the presence of $\eta = -\sigma_1$. More precisely, we will consider this system with $\sigma_1 \ll 1$ and, separately, with $\sigma_1 \gg 1$. In the latter case, we use $\sigma_2 = 1/\sigma_1$ as the singular parameter. Then we complete the proof for $\sigma_1 = O(1)$ using the theory of rotating of vector fields.

When $\sigma_1 \ll 1$, this system is a singular perturbation of

$$\begin{aligned} u_1' &= 0, \\ v_1' &= \frac{\gamma v_1}{1 + \alpha v_1} - u_1 v_1. \end{aligned} \tag{3.2}$$

The sets

$$L_1(\sigma_1 = 0) = \{(u_1, v_1), v_1 = 0\} \tag{3.3}$$

and

$$L_2(\sigma_1 = 0) = \{(u_1, v_1), v_1 = \frac{\gamma - u_1}{\alpha u_1}\} \tag{3.4}$$

are lines of equilibria for the fast system (3.2). For each $u_1 = u_1^* < \gamma$, the equilibrium $(u_1^*, 0)$ of (3.2) has a one-dimensional central manifold and a one-dimensional unstable manifold (corresponding to the positive eigenvalue $\gamma - u_1^*$). On the other hand, for each $u_1 = u_1^* < \gamma$, the equilibrium $(u_1^*, \frac{\gamma - u_1^*}{\alpha u_1^*})$ that belongs to $L_2(\sigma_1 = 0)$ has a one-dimensional central manifold and a one-dimensional stable manifold. The portion of the curve $L_2(\sigma_1 = 0)$ that corresponds to $u_1 < \gamma$ has then a two-dimensional stable manifold which intersects with a one-dimensional unstable manifold of each $(u_1^*, 0)$ transversally (by dimension counting). Therefore, for each fixed $u_1 = u_1^*$, there is a fast connection that connects $(u_1^*, 0)$ to the point $(u_1^*, \frac{\gamma - u_1^*}{\alpha u_1^*}) \in L_2(\sigma_1 = 0)$.

The slow flow on the set $L_2(\sigma_1 = 0)$ is given by

$$\dot{u}_1 = -(1 - \frac{1}{\alpha})u_1 - \frac{\gamma}{\alpha} + 1. \tag{3.5}$$

Equation (3.5) has one stable (since $\alpha > 1$) equilibrium that corresponds to equilibrium B of the full system. On $\{v_2 = 0\}$-plane there is then a singular orbit between A and B that

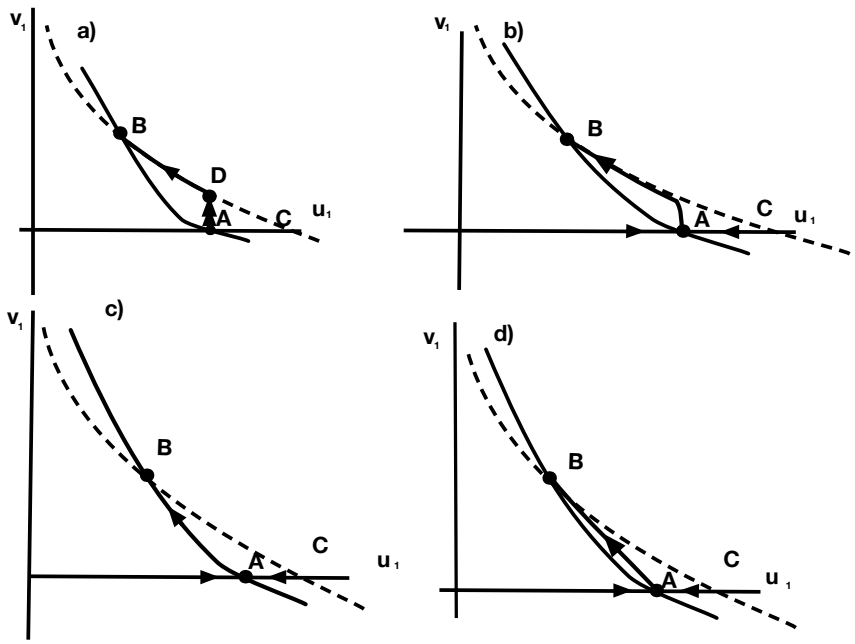

Figure 3.1. *Region 1: a) Singular wave, $\sigma_1 = 0$. b) Wave in the perturbed system, $\sigma_1 \ll 1$. c) Singular wave, $\sigma_2 = 0$. d) Wave in the perturbed system, $\sigma_2 \ll 1$. The dashed curve is $\Gamma_3 = \{(\gamma/(1+\alpha v_1), v_1, 0)\}$ and the solid curve is $\Gamma_1 = \{(1/(1+v_1), v_1, 0)\}$.*

consists of two pieces: a fast piece that connects the equilibrium $A = (1, 0, 0)$ to the point $D = (1, \frac{\gamma-1}{\alpha}, 0)$ that belongs to $L_2(\sigma_1 = 0)$ and a slow piece that connects D to the equilibrium A. See Figure 3.1, panel a) for the illustration.

Because of the transversality of the intersection, this orbit persists upon switching on $\sigma_1 \ll 1$ (see Figure 3.1, panel b)). More precisely, there exists a $\tilde{\sigma}_1$ such that for any $0 < \sigma_1 \leq \tilde{\sigma}_1$ there exits a heteroclinic orbit.

Moreover, for fixed parameters σ_1, γ, and α there is a small enough $n\epsilon_0 > 0$ such that for each $\epsilon < \epsilon_0$ this orbit persists as a solution of the full system (2.5) that connects the saddle at A to the stable equilibrium B as implied by the Geometric Singular Perturbation Theory ([7], [9]).

Next we consider the singular limit $\sigma_2 = 1/\sigma_1 \ll 1$. The system (3.1) is then singularly perturbed with the small parameter σ_2. After rescaling the system (2.8) reads

$$\begin{aligned} u_1' &= -(v_1 u_1 - 1 + u_1), \\ v_1' &= \sigma_2 (\frac{\gamma v_1}{1 + \alpha v_1} - u_1 v_1). \end{aligned} \tag{3.6}$$

We note that we use the same notation for the derivatives here and in the systems above although they are taken with respect to the appropriate, different coordinates.

We let $\sigma_2 \to 0$ and obtain the fast reduced system

$$\begin{aligned} u_1' &= -(v_1 u_1 - 1 + u_1), \\ v_1' &= 0. \end{aligned} \tag{3.7}$$

The set $L_3(\sigma_2 = 0) = \{(u_1, v_1), u_1 = \frac{1}{v_1+1}\}$ is a line of equilibria for the limiting system (3.7). The slow flow on $L_3(\sigma_2 = 0)$ is given by

$$\dot{v}_1 = \frac{\gamma v_1}{1 + \alpha v_1} - \frac{v_1}{v_1 + 1}.$$

The set $L_3^+(\sigma_2 = 0) = \{(u_1, v_1), u_1 = \frac{1}{v_1+1}, v_1 > 0\}$ is normally hyperbolic, and attracting invariant set for (3.7). Indeed, linearization of (3.7) around each equilibria $(\frac{1}{v_1^*+1}, v_1^*)$ has a zero eigenvalue and an eigenvalue $-1 - v_1^*$. Under small perturbations it persists as an invariant manifold $L_3(\sigma_2)^+$ for (3.7). The slow flow on the perturbed normally hyperbolic invariant set $L_3(\sigma_2)^+$ is given by

$$\dot{v}_1 = \frac{v_1(v_1(\gamma - \alpha) - 1 + \gamma)}{(1 + \alpha v_1)(v_1 + 1)} + O(\sigma_2). \tag{3.8}$$

This equation of first order possesses one unstable equilibrium that corresponds to the saddle equilibrium A in the full system and one stable equilibrium that corresponds to the equilibrium B and a solution that connects them. The solution that connects equilibria of (3.8) corresponds to the heteroclinic orbit of (3.1) that connects A to B which is near $L_3(\sigma_2 = 0)$. More precisely, there exists a $\tilde{\sigma}_2$ such that for any $\sigma_2 \le \tilde{\sigma}_2$ (alternatively, $\sigma_1 \ge \tilde{\tilde{\sigma}}_1 = 1/\tilde{\sigma}_2$) there exits an orbit that asymptotically connects A to B (see Figure 3.1 b)).

Dimension counting shows that this orbit persists as a solution of the full system when is $\epsilon \ll 1$ as implied by the Geometric Singular Perturbation Theory.

Existence of traveling waves at and near limits when $\sigma_1 = |\eta| \to 0$ and $\sigma_2 = 1/\sigma_1 \to 0$ are local results - they hold for sufficiently small and sufficiently large values of σ_1. The existence of the waves for every σ_1 follows from the theory of rotation vector fields [5], [12] and a "trapping region" type argument.

We think of (3.1) (or, alternatively, (3.6)) as a two-dimensional dynamical system with planar vector field generated by $F = (f_1, f_2)$, where $f_1(u_1, v_1) = -\sigma_1(v_1 u_1 - 1 + u_1)$ and $f_2(u_1, v_1) = \frac{\gamma v_1}{1+\alpha v_1} - u_1 v_1$. Note that the nullclines of this system (and, therefore, the equilibria themselves) are independent of the parameter σ_1. Denote the angle between the u_1-axis and the vector $F(u_1, u_2)$ by

$$\theta(u_1, v_1) = \tan^{-1} \frac{f_2(u_1, v_1)}{f_1(u_1, v_1)}.$$

At each point (u_1, v_1), $\frac{\partial \theta}{\partial \sigma_1}$ measures the rate of change of θ as a function of σ_1. In our case,

$$\frac{\partial \theta}{\partial \sigma_1} = \frac{f_1 \frac{\partial f_2}{\partial \sigma_1} - f_2 \frac{\partial f_1}{\partial \sigma_1}}{f_1^2 + f_2^2} = -\frac{v_1(1 + v_1)\left(u_1 - \frac{1}{1+v_1}\right)\left(u_1 - \frac{\gamma}{1+\alpha v_1}\right)}{\sigma_1^2(u_1(v_1 + 1) - 1)^2 + \left(\frac{\gamma}{1+\alpha v_1} - u_1\right)^2 v_1^2} \tag{3.9}$$

is positive in the region bounded by the nullclines and the u_1-axis. So as σ_1 increases the vector field in that region rotates counterclockwise. The system (3.1) (and, similarly, (3.6)) defines a rotating vector field [5], [12]. This, in part, implies that the waves in both singular limit cases $\sigma_1 = 0$ and $\sigma_1 = \infty$ ($\sigma_2 = 0$) perturb to waves that entirely belong to the region bounded by the nullclines and the u_1-axis.

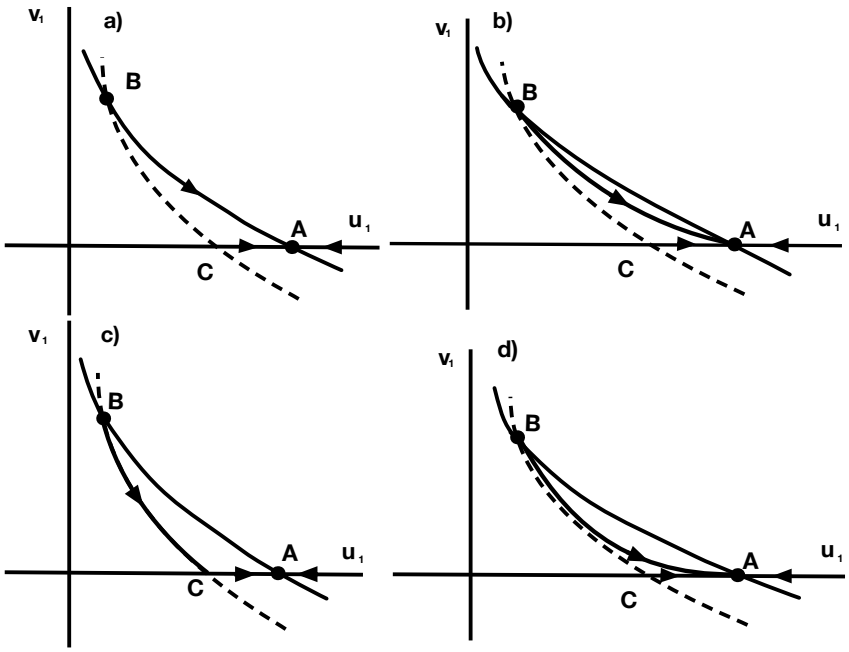

Figure 3.2. *When parameters belong to Region 2, A is an attractor and B is a saddle. The unstable manifold of B rotates between the two singular positions. a) Singular wave, $\sigma_1 = \infty$. b) Wave in the perturbed system, $\sigma_1 \gg 1$. c) Singular wave, $\sigma_1 = 0$. d) Wave in the perturbed system, $\sigma_1 \ll 1$. The dashed curve is $\Gamma_3 = \{(\gamma/(1+\alpha v_1), v_1, 0)\}$ and the solid curve is $\Gamma_1 = \{(1/(1+v_1), v_1, 0)\}$.*

Next we consider the case when $\sigma_1 = O(1)$. Recall that we work with (3.1) with fixed values of parameters γ and α. Let σ_1 be a value $\tilde{\sigma}_1 < \sigma_1 < \tilde{\tilde{\sigma}}_1$. The stable manifold $W^u(A)(\sigma_1)$ of the equilibrium A is then located between the stable manifolds of A with $\tilde{\sigma}_1$ and $\tilde{\tilde{\sigma}}_1$. It was proved in [12, Section 2, Precession of Saddle Separatrices] that, as σ_1 increases within interval $[\tilde{\sigma}_1, \tilde{\tilde{\sigma}}_1]$, the saddle separatrices (here solutions that follow $W^s(A)(\sigma_1)$) (a) move monotonically counterclockwise along transversals (i.e. along each sufficiently small circle centered at the saddle point A) from the initial position to the final position which is the orbit that corresponds to $\tilde{\tilde{\sigma}}_1$; (b) never self-intersect, i.e. $W^s(A)(\sigma_1^*) \cap W^s(A)(\sigma_1^{**}) = \emptyset$, for $\sigma_1^* \neq \sigma_1^{**}$. Therefore the orbit that follows $W^s(A)(\sigma_1)$ for any $\sigma_1 \in [\tilde{\sigma}_1, \tilde{\tilde{\sigma}}_1]$ will have to enter the only other equilibrium in that region, equilibrium B, thus creating a heteroclinic orbit. This completes the proof of the existence of the traveling waves for the Region 1.

The argument used above can be viewed as non-traditional "trapping region" type argument, since the boundaries of the region (orbits for $\tilde{\sigma}_1$ and $\tilde{\tilde{\sigma}}_1$) exist not for the same parameters as the solution that is considered (some fixed $\sigma_1 \in [\tilde{\sigma}_1, \tilde{\tilde{\sigma}}_1]$) but nevertheless serve as obstructions for the solution that prevent it from leaving the region.

3.2. Region 2: $0 < \alpha < \gamma < 1$, $\eta < 0$.. Theorem 3.4. *For each fixed α, η, γ from Region 2, there exists $\epsilon_0 = \epsilon_0(\alpha, \eta, \gamma) > 0$ such that for any $\epsilon < \epsilon_0$ there is a heteroclinic orbit that asymptotically connects B to A.*

In this parameter regime the equilibrium $A = (1, 0, 0)$ is strictly to the right of the point

$C = (\gamma, 0, 0)$ on the plane $v_2 = 0$ (see Figure 3.2).

Recall that we consider the reduced system (3.1)

$$u_1' = -\sigma_1(v_1 u_1 - 1 + u_1),$$
$$v_1' = \frac{\gamma v_1}{1 + \alpha v_1} - u_1 v_1,$$

where $\sigma_1 = |\eta|$. In the limit $\sigma_1 \to 0$ this system becomes (3.2). The limiting system has two curves of equilibria: $L_2(\sigma_1 = 0) = \{(u_1, v_1), v_1 = \frac{\gamma - u_1}{\alpha u_1}\}$ and $L_1(\sigma_1 = 0) = \{(u_1, v_1), v_1 = 0\}$. If we linearize the limiting system around each of these equilibria, we see that the portions of $L_1(\sigma_1 = 0)$ and $L_2(\sigma_1 = 0)$ that we are interested in have useful properties: $L_1^{\mathrm{R}}(\sigma_1 = 0) = \{(u_1, v_1), v_1 = 0, u_1 < \gamma\}$ is normally repelling, while $L_2^{\mathrm{R}}(\sigma_1 = 0) = \{(u_1, v_1), v_1 = 0, u_1 > \gamma\}$ and $L_2^{+}(\sigma_1 = 0) = \{(u_1, v_1), v_1 = \frac{\gamma - u_1}{\alpha u_1}, v_1 > 0\}$ are normally attracting. The equilibrium at B is a saddle and has a one-dimensional unstable manifold $W^u(B)$. On the other hand, A has two-dimensional stable manifold and is a stable node. The solution that leaves B does so along $W^u(B)$ which happens to be the nullcline $L_2(\sigma_1 = 0)$ and after reaching point C switches to follow the line $v_1 = 0$ which is an invariant set for both (3.1) and the limiting system (3.2).

There exists then a singular heteroclinic orbit that connects B to A. It consists of two slow pieces: a piece that is the segment of L_2^{+} that connects B to C and the second piece which is the segment of L_1^{R} that connects C to A. Note that L_1^{R} is an invariant set for the system (3.1) too. The rotation of the saddle separatrix of B then implies the existence of the heteroclinic orbit that connects B to A in (3.1). More details will follow after the discussion of the second singular wave. By the Geometric Singular Perturbation Theory, when σ_1 is sufficiently small, that heteroclinic orbit is near the singular orbit (see Figure 3.2).

Next we consider the reduced system (3.6) which has a fast-slow structure with respect a small parameter $\sigma_2 = 1/|\eta| \ll 1$. The system (3.6) in the limit $\sigma_2 \to 0$,

$$u_1' = -(v_1 u_1 - 1 + u_1),$$
$$v_1' = 0, \tag{3.10}$$

has a curve of equilibria $\{(u_1, v_1),\ u_1 = \frac{1}{v_1 + 1}\}$. Linearization of (3.10) around each of these equilibria, say $(\frac{1}{v_1^* + 1}, v_1^*)$, has a zero eigenvalue and, for $v_1^* > 0$, and a negative eigenvalue equal to $-(v_1^* + 1)$. Therefore, the set of equilibria is normally hyperbolic and attracting when $v_1 > 0$. By the Geometric Singular Perturbation Theory, it persists as an invariant set for the system (3.6) for sufficiently small σ_2. The reduced flow on the perturbed normally hyperbolic manifold $\{(u, v), v_1 = \frac{1}{v_1 + 1} + O(\sigma_2)\}$ is given by

$$\dot{v}_1 = \frac{v_1(v_1(\gamma - \alpha) - 1 + \gamma)}{(1 + \alpha v_1)(v_1 + 1)} + O(\sigma_2). \tag{3.11}$$

It possesses a connection between $v_1 = \frac{\gamma - 1}{\alpha - \gamma}$, which corresponds to the saddle equilibrium B of the full system, and $v_1 = 0$, which corresponds to stable equilibrium A. This solution persists upon switching on the parameter σ_2.

The same way as in Section 3.1, for ϵ sufficiently small, both singular orbits perturb to heteroclinic orbits for the full system (2.4).

Arguments similar to the ones used in Section 3.1 also show that the heteroclinic orbit between the two fixed points B and A rotates monotonically counterclockwise around the saddle equilibrium at B when $\sigma_1 = |\eta|$ changes from 0 to ∞, because $\frac{\partial\theta}{\partial\sigma_1}$ is positive in Region 2, according to formula (3.9). Therefore both of the orbits, one that corresponds to the perturbation by small $\sigma_1 \le \tilde{\sigma}_1$ and the one that corresponds to the perturbation by small $\sigma_2 = 1/\sigma_1$ ($\sigma_1 \ge \tilde{\tilde{\sigma}}_1$), entirely belong to the region bounded by the nullclines and the v_1 -axis. For any $\sigma_1 \in (\tilde{\sigma}_1, \tilde{\tilde{\sigma}})$, the orbit that leaves the equilibrium at B is trapped by these two orbits and therefore has to converge to the equilibrium at A.

3.3. Region 3: $1 < \gamma < \alpha$, $\eta > 0$. Theorem 3.5. *For each fixed α, η, γ from Region 3, there exists $\epsilon_0 = \epsilon_0(\alpha, \eta, \gamma) > 0$ such that for any $\epsilon < \epsilon_0$ there is a heteroclinic orbit that connects a saddle B to an unstable node A.*

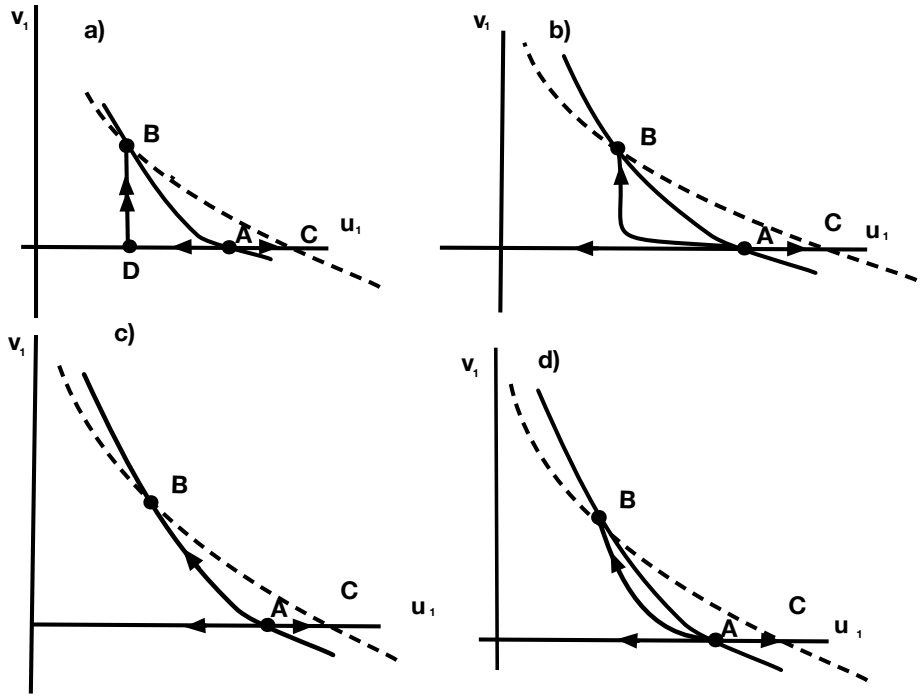

Figure 3.3. *Region 3: A is a repeller, B is a saddle. a) Singular wave, $\eta = 0$. b) Wave in the perturbed system, $\eta \ll 1$. c) Singular wave, $1/\eta = 0$. d) Wave in the perturbed system, $1/\eta \ll 1$. The dashed curve is $\Gamma_3 = \{(\gamma/(1+\alpha v_1), v_1, 0)\}$ and the solid curve is $\Gamma_1 = \{(1/(1+v_1), v_1, 0)\}$.*

The analysis of the heteroclinic orbits connecting A and B in the Region 3 is similar to the analysis of the heteroclinic orbits in Region 1. The construction of the first singular wave does not depend on the sign of η as η is set to zero. When η is sufficiently small the equilibria are of the nature different from ones they have in Region 1: the equilibrium at A is now an unstable node (it is a saddle in Region 1), and the equilibrium at B is a saddle (B is a stable node in Region 1). The construction of the second limiting wave at $\eta \to \infty$ is also analogous. When η is sufficiently small and sufficiently large, the perturbed waves exists and can be used as boundaries of the "trapping" region. Using calculations similar to (3.9) for Region 4 it is

easy to see that the separatrix of the saddle (here, B) rotates clockwise, therefore the same arguments as in Section 3.1 imply existence of the heteroclinic orbit for any $\eta > 0$. That connection persists when a sufficiently small ϵ is introduced in the problem (see equations (2.5)). Since all of the arguments are essentially similar to ones presented in Section 3.1, we omit the details and illustrate the situation in Figure 3.3.

4. Existence of a periodic orbit.

4.1. Regime 4.

Concerning the existence of a periodic orbit the following results hold.

Theorem 4.1. *Assume that α and γ are such that $0 < \alpha < \gamma < 1$. Then in the system (2.8), the equilibrium B undergoes a Hopf bifurcation at*

$$\eta_H = \frac{\alpha(\gamma-1)(\alpha-\gamma)^2}{(\alpha-1)^3\gamma}.$$

Furthermore, there is $\alpha_0 = \alpha_0(\gamma) > 0$ such that if $\alpha < \alpha_0$ then the Hopf bifurcation is subcritical and for $\eta \in (\eta_H - h, \eta_H)$, where $0 < h \ll 1$, there exist

i) a periodic orbit around the equilibrium B,
ii) a heteroclinic orbit of (2.5) that asymptotically connects a periodic orbit around B with the equilibrium A,
iii) a manifold of heteroclinic orbits that asymptotically connect the equilibrium at B with the periodic orbit around B.

Moreover, there exists $\epsilon_0 = \epsilon_0(\alpha, \gamma, \eta) > 0$ such that these orbits persist in the system (2.5) for $\epsilon < \epsilon_0$.

Remark 4.2. *Whether the periodic orbit around the equilibrium B in (2.8) is unique is an open question.*

The proof of Theorem 4.1 uses the analysis of the behavior of the reduced system (2.8) near infinity using Poincaré compactification and Poincaré-Bendixson theorem.

The occurrence of a subcritical Hopf bifurcation follows from the classic Hopf Bifurcation Theorem (see for example, [1, pp. 261-264], or [12, 352]). To claim the conclusions of Theorem 4.1 for system (2.8), we calculate the Lyapunov number. Recall (see [1, p.253]) that for a planar vector field defined by an analytic system,

$$\begin{aligned} \dot{x} &= ax + by + p(x,y), \\ \dot{y} &= cx + dy + q(x,y), \end{aligned}$$

with

$$\Delta = ad - bc > 0, \quad a + d = 0, \quad p(x,y) = \sum_{j+j\geq 2} a_{ij}x^i y^j, \quad q(x,y) = \sum_{j+j\geq 2} b_{ij}x^i y^j,$$

the Lyapunov number is given by the formula

$$\begin{aligned} \sigma = &\frac{-3\pi}{2b\Delta^{3/2}}\{[ac(a_{11}^2 + a_{11}b_{02} + a_{02}b_{11}) + ab(b_{11}^2 + a_{20}b_{11} + a_{11}b_{02}) + c^2(a_{11}a_{02} + 2a_{02}b_{02}) \\ &-2ac(b_{02}^2 - a_{20}a_{02}) - 2ab(a_{20}^2 - b_{20}b_{02}) - b^2(2a_{20}b_{20} + b_{11}b_{20}) + (bc - 2a^2)(b_{11}b_{02} \\ &-a_{11}a_{20})] - (a^2 + bc)[3(cb_{03} - ba_{30}) + 2a(a_{21} + b_{12}) + (ca_{12} - bb_{21})]\}. \end{aligned}$$

To perform this calculation in our case, we first notice that on the closed upper half-plane $\{(u_1, v_1),\ v_1 \geq 0\}$, the system (2.8) is topologically equivalent to

$$\begin{aligned} u_1' &= \eta(\alpha v_1 + 1)(v_1 u_1 - 1 + u_1), \\ v_1' &= v_1(\gamma - u_1(1 + \alpha v_1)), \end{aligned} \tag{4.1}$$

via coordinate transformation

$$\zeta = \int_0^{\xi} \frac{1}{1 + \alpha v_1}\, ds.$$

As before, with an abuse of notation, we use $'$ to denote the derivative with respect the new variable ξ. It is also clear that the equilibrium of (2.8) can be shifted to the origin by a linear transformation. The new system generates a polynomial vector field for which the formula for the Lyapunov number σ is applicable. It yields an expression that us not so inconvenient for the analysis:

$$\sigma = \frac{\pi}{P(\alpha, \gamma)} G(\alpha, \gamma),$$

where

$$P(\alpha, \gamma) = 1.5\gamma(1 - \alpha)(1 - \gamma)(\gamma - \alpha)^2 \sqrt{\alpha(\gamma - \alpha)},$$

and

$$\begin{aligned} G(\alpha, \gamma) =& -\alpha^6 + (2\gamma + 1)\alpha^5 + (\gamma^2 - 2\gamma - 3)\alpha^4 \\ & -(2\gamma^3 + 3\gamma^2 - 6\gamma - 3)\alpha^3 + (\gamma^4 + 3\gamma^2 - 6\gamma - 1)\alpha^2 + (2\gamma - \gamma^2)\alpha. \end{aligned}$$

We note that $P(\alpha, \gamma) > 0$ within this regime, $G(0, \gamma) = 0$, and $\frac{\partial G}{\partial \alpha}(0, \gamma) = \gamma(2 - \gamma) > 0$ when $0 < \gamma < 1$. Therefore, for each fixed γ there are values of α sufficiently small to guarantee that the Lyapunov number σ is positive. Therefore the equilibrium B is nonlinearly unstable when $\eta = \eta_H$ and, as η passes through η_H, B generates an unstable limit cycle, and thus B undergoes a subcritical Hopf bifurcation. The existence of an orbit that connects a closed orbit around B to the equilibrium A follows from the Poincaré-Bendixson theorem and the compactification.

4.2. Compactification. In this section instead of (2.8) we continue to work with the topologically equivalent on $\{(u_1, v_1),\ v_1 \geq 0\}$ system (4.1). To map the upper hemisphere of the Poincaré sphere $\mathbb{S}^2$ onto the (u_1, v_1)-plane, one introduces a coordinate transformation $u_1 = X/Z$, $v_1 = Y/Z$. Then

$$X = \frac{u_1}{\sqrt{1 + u_1^2 + v_1^2}}, \quad Y = \frac{v_1}{\sqrt{1 + u_1^2 + v_1^2}}, \quad Z = \frac{1}{\sqrt{1 + u_1^2 + v_1^2}}. \tag{4.2}$$

The points on the equator $X^2 + Y^2 = 1$ on the Poincaré sphere correspond to the infinity of the (u_1, v_1)-plane. Since

$$du_1 = \frac{Z dX - X dZ}{Z^2}, \quad dv_1 = \frac{Z dY - Y dZ}{Z^2},$$

the induced flow on the Poincaré sphere is given by the following differential form [2, 13]:

$$Zf_2(\frac{X}{Z},\frac{Y}{Z})dX - Zf_1(\frac{X}{Z},\frac{Y}{Z})dY + (Yf_1(\frac{X}{Z},\frac{Y}{Z}) - Xf_2(\frac{X}{Z},\frac{Y}{Z}))dZ = 0, \tag{4.3}$$

where

$$f_1(u_1,v_1) = \eta(\alpha v_1 + 1)(-1 + u_1 + u_1 v_1),$$
$$f_2(u_1,v_1) = v_1(\gamma - u_1(1+\alpha v_1)).$$

We desingularize (4.3) and look for the critical points on the equator of the Poincaré sphere. These critical points correspond to critical points of the original system at infinity and can be found by setting $Z = 0$ in the desingularized version of (4.3), which then reads

$$-\alpha Y^2 X(Y\eta + X) = 0. \tag{4.4}$$

We solve this equation under the conditions $X^2 + Y^2 = 1$ and $Y \geq 0$ and obtain four critical points $E_1 = (-1,0)$, $E_2 = (-\eta/\sqrt{1+\eta^2}), 1/\sqrt{1+\eta^2})$, $E_3 = (0,1)$, and $E_4 = (1,0)$. We are interested in the flow near the critical points at infinity. According to [3] the flow on the equator in polar coordinates is given by the first order differential equation

$$\dot{\theta} = -\alpha \sin^2(\theta)\cos(\theta)(\sigma\sin(\theta) + \cos(\theta)). \tag{4.5}$$

The flow on the upper-half plane is schematically shown on Figure 4.1. Since the degree of the polynomial vector field, which is the maximum of the degrees of the polynomials $f_1(u_1,v_1)$ and $f_2(u_1,v_1)$, is 3 (an odd number), the antipodal critical points at infinity are qualitatively equivalent [6, 2]. We carry out the analysis of the equilibria at infinity by considering the flow on the following three local charts of the Poincaré sphere:

$$U_y^+ = \{(x,y,z) \in \mathbb{S}^2 | y > 0\}, \quad U_x^+ = \{(x,y,z) \in \mathbb{S}^2 | x > 0\}, \quad U_x^- = \{(x,y,z) \in \mathbb{S}^2 | x < 0\}.$$

Using the third chart U_x^- makes it easier to determine the flow on the upper half-plane near the degenerate equilibrium at the intersection of the equator and the x-axis.

To analyze E_2 and E_3, we project the flow on the local chart $U_y^+ = \{(x,y,z) \in \mathbb{S}^2 | y > 0\}$ onto the plane $Y = 1$,

$$\begin{aligned} \dot{x} &= \alpha x^2 + \eta\alpha x - \eta z^3 + (-\eta\alpha + \eta x - \gamma x)z^2 + (\eta\alpha x + x^2 + \eta x)z, \\ \dot{z} &= z(-\gamma z^2 + \alpha x + xz). \end{aligned} \tag{4.6}$$

The points E_2 and E_3 are in bijective correspondence with points $\tilde{E}_2 = (x,z) = (-\eta, 0)$ and $\tilde{E}_1 = (x,z) = (0,0)$, respectively, on $Y = 1$ plane.

The linearization of the system (4.6) at $\tilde{E}_2$ has a double negative eigenvalue $\lambda_{1,2} = -\alpha\eta$, therefore $\tilde{E}_2$ is a hyperbolic equilibrium and is an attractor.

The linearization of (4.6) at $\tilde{E}_3$ has a zero eigenvalue and an eigenvalue which is equal to $\alpha\eta$ that corresponds to the flow on the equator. In order to determine the nature of this equilibrium, we study the flow restricted to the local center manifold

$$W^c(E_3) = \{(x,z) | x = z^2 + \mathrm{O}(z^3)\}, \tag{4.7}$$

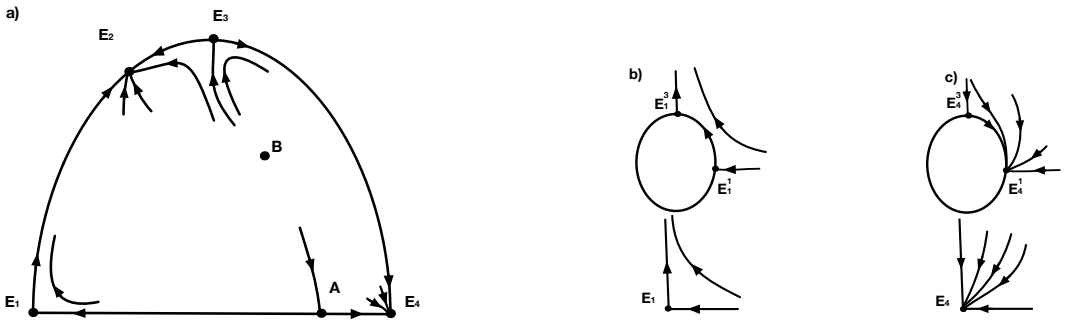

Figure 4.1. *a) The flow on the equator and near the singular points in the closed upper half-plane. b) The flow near the equilibrium E_1. c) The flow near the equilibrium E_4.*

which is given by the following equation

$$\dot{z} = (\alpha - \gamma)z^3 + \mathrm{O}(z^3). \tag{4.8}$$

Since $\alpha < \gamma$ within this region and we are interested in the flow that corresponds to the top of the sphere ($z \geq 0$), we conclude that $\tilde{E}_3$ is a saddle.

To analyze the behavior of the equilibrium E_1 we project the vector field on local chart $U_x^+ = \{(x, y, z) \in \mathbb{S}^2 | x > 0\}$ of the Poincaré sphere onto the plane $X = 1$, thus obtaining

$$\begin{aligned} \dot{y} &= -\alpha y^2(\eta y + 1) + \eta y z^3 - y(-\eta\alpha y - \gamma + \eta)z^2 - y(1 + \eta\alpha y + \eta y)z, \\ \dot{z} &= -\eta z(\alpha y + z)(-z^2 + z + y). \end{aligned} \tag{4.9}$$

On this local chart, the point E_1 is represented by the point $\tilde{E}_1 = (y, z) = (0, 0)$. Note that the linearization of (4.9) about the point $\tilde{E}_1$ is identically equal to zero, so $\tilde{E}_1$ (and, thus, E_1) is a degenerate equilibrium. To study this degenerate equilibrium of (4.9) at the origin, we perform the quasi-homogeneous blow-up with the coordinate transformation

$$\phi : \mathbb{S}^1 \times \mathbb{R} \to \mathbb{R}^2, \quad ((\bar{z}, \bar{y}), r) \mapsto (z, y), \tag{4.10}$$

where $\bar{z}^2 + \bar{y}^2 = 1$ and

$$z = r\bar{z}, \quad y = r\bar{y}. \tag{4.11}$$

We use charts on $\mathbb{S}^1$ to calculate the flow near E_4 on the top of the sphere ($z \geq 0$) that corresponds to the upper half plane ($y \geq 0$). At first we consider the directional blow-up

$$z = r, \quad y = r\bar{y}, \tag{4.12}$$

in the $z > 0$ direction. In the blow-up coordinates (4.12), differential equations (4.9) become

$$\begin{aligned} \dot{r} &= r^3\eta(-1 - \bar{y} + r)(1 + \alpha\bar{y}), \\ \dot{\bar{y}} &= -r\bar{y}(-\gamma r + 1 + \alpha\bar{y}). \end{aligned} \tag{4.13}$$

An appropriate rescaling of the independent variable leads to the following system

$$\begin{aligned} \dot{r} &= r^2\eta(-1-\bar{y}+r)(1+\alpha\bar{y}),\\ \dot{\bar{y}} &= -\bar{y}(-\gamma r+1+\alpha\bar{y}). \end{aligned} \tag{4.14}$$

The system (4.14) has two equilibria: $E_4^1(0,0)$ with eigenvalues 0 and -1 and $E_4^2(0,-\frac{1}{\alpha})$ with eigenvalues 0 and 1. We will not consider $E_4^2(0,-\frac{1}{\alpha})$ since its nature determines the flow in the lower half-plane. However, the semi-hyperbolic equilibrium $E_4^1(0,0)$ is of interest to us. It corresponds to the intersection point of the equator and the positive x-axis. On the invariant line $\bar{y}=0$, the system (4.14) becomes $\dot{r}=-r^2$, which corresponds to the flow on the positive x-axis. When $r=0$, the flow of (4.14) is given by $\dot{\bar{y}}=-\bar{y}(1+\alpha\bar{y})$ which shows that the equilibrium $E_4^1(0,0)$ is attracting along the blown-up circle within the first quadrant.

Next we use directional blow up coordinates

$$z=r\bar{z},\quad y=r, \tag{4.15}$$

to blow-up the origin in the $y>0$ direction. With (4.15) the differential equations (4.9) become

$$\begin{aligned} \dot{\bar{z}} &= r\bar{z}(-\gamma r\bar{z}^2+\bar{z}+\alpha),\\ \dot{r} &= -r^2(z+\alpha-(-\alpha\eta\bar{z}+\gamma\bar{z}^2-\eta\bar{z}^2-\eta\bar{z}-\alpha\eta)r-\alpha(\eta\alpha\bar{z}^2+\eta\bar{z}^3)r^2). \end{aligned} \tag{4.16}$$

We then desingularize (4.16) by rescaling with respect to the independent variable to obtain

$$\begin{aligned} \dot{\bar{z}} &= \bar{z}(-\gamma r\bar{z}^2+\bar{z}+\alpha),\\ \dot{r} &= -r(z+\alpha-(-\alpha\eta\bar{z}+\gamma\bar{z}^2-\eta\bar{z}^2-\eta\bar{z}-\alpha\eta)r-\alpha(\eta\alpha\bar{z}^2+\eta\bar{z}^3)r^2). \end{aligned} \tag{4.17}$$

The system (4.17) has an equilibrium at $E_4^3(0,0)$ which is a saddle with eigenvalues $\pm\alpha$ and a semi-hyperbolic equilibrium at $E_4^4(-\alpha,0)$ which is not relevant to the flow in the first quadrant of the vector field. The direct examination of (4.17) shows that the equilibrium $E_4^3(0,0)$ is attracting along the invariant line $\bar{z}=0$, which corresponds to the flow on the equator, and it is repelling along the line $r=0$, which is consistent with our analysis above. Combining the information obtained from the analysis of the flow on these two charts we conclude that there is a stable parabolic sector at E_4 that belongs to the upper-half plane (see Figure 4.1, panels c) and a)).

To study E_1, we use another local chart. More precisely, the flow projected from the local chart $U_x^- = \{(x,y,z)\in\mathbb{S}^2 | x<0\}$ of the Poincaré sphere onto the plane $X=-1$ is given by

$$\begin{aligned} \dot{y} &= -\eta yz^3+(-\alpha\eta y^2-\eta y+\gamma y)z^2+(-\alpha\eta y^2-\eta y^2+y)z-\alpha\eta y^3+\alpha y^2,\\ \dot{z} &= -\alpha\eta zy^2+(-\alpha\eta z^3-\alpha\eta z^2-\eta z^2)y-\eta z^4-\eta z^3. \end{aligned} \tag{4.18}$$

Note that the point E_1, which is the antipodal point to E_4 is a degenerate equilibrium with zero linear part , as expected. To analyze the flow near E_1 on the upper half-plane, we perform the quasi-homogeneous blow-up with the coordinate transformation (4.11). We consider the

directional blow-up (4.15) in the $y > 0$ direction. The differential equations (4.18) in these coordinates become

$$\begin{aligned} \dot{r} &= -r^2(\alpha\eta r^2\bar{z}^2 + \eta r^2\bar{z}^3 + \alpha\eta r\bar{z} + \eta r\bar{z}^2 - \gamma r\bar{z}^2 + \alpha\eta r + \eta r\bar{z} - \alpha - \bar{z}), \\ \dot{\bar{z}} &= -r\bar{z}(\gamma r\bar{z}^2 + \alpha + \bar{z}). \end{aligned} \tag{4.19}$$

We rescale the independent variable in (4.19) by r and obtain

$$\begin{aligned} \dot{r} &= -r(\alpha\eta r^2\bar{z}^2 + \eta r^2\bar{z}^3 + \alpha\eta r\bar{z} + \eta r\bar{z}^2 - \gamma r\bar{z}^2 + \alpha\eta r + \eta r\bar{z} - \alpha - \bar{z}), \\ \dot{\bar{z}} &= -\bar{z}(\gamma r\bar{z}^2 + \alpha + \bar{z}). \end{aligned} \tag{4.20}$$

The system (4.20) has a saddle equilibrium $E_1^1 = (0,0)$ with eigenvalues $\pm\alpha$ and $E_1^2 = (0,-\alpha)$ with eigenvalues 0 and 1 that correspond to the equilibria on the blown-up circle. Equilibrium $E_4^1(0,0)$ is attracting along the line $\bar{z} = 0$. The flow of (4.20) restricted to the invariant line $r = 0$ is given by $\dot{\bar{z}} = -\bar{z}(\alpha + \bar{z})$, therefore E_1^1 is attracting along this line. This information extends to the flow on the sector of the blown-up circle that belongs to the first quadrant. The equilibrium E_1^1 is repelling along the line $\bar{z} = 0$ due to the reduced flow $\dot{r} = \alpha r$ that implies the behavior of the flow on the equator of the Poincaré sphere.
Next we use directional blow up coordinates (4.12) to blow-up the origin in the $z > 0$ direction. With (4.12) the differential equations (4.18) become

$$\begin{aligned} \dot{\bar{y}} &= r\bar{y}(\alpha\bar{y} + \gamma r + 1), \\ \dot{r} &= -r^3\eta(\alpha r\bar{y} + \alpha\bar{y}^2 + \alpha\bar{y} + r + \bar{y} + 1). \end{aligned} \tag{4.21}$$

We desingularize the system (4.21) by rescaling with respect to the independent variable and obtain

$$\begin{aligned} \dot{\bar{y}} &= \bar{y}(\alpha\bar{y} + \gamma r + 1), \\ \dot{r} &= -r^2\eta(\alpha r\bar{y} + \alpha\bar{y}^2 + \alpha\bar{y} + r + \bar{y} + 1). \end{aligned} \tag{4.22}$$

We consider only the equilibrium $E_1^3 = (0,0)$ of this system. It is semi-hyperbolic with eigenvalues 1, 0. The flow of (4.22) on the invariant line $\bar{y} = 0$, which corresponds to the x-axis, is given by $\dot{r} = -\eta r^2(1 + r)$, therefore E_1^3 is attracting along this line. The flow on the invariant line $r = 0$ corresponds to the flow on the segment of the blown-up circle that connects E_1^3 to E_1^1 and is given by $\dot{\bar{y}} = \bar{y}(1 + \alpha\bar{y})$ which is consistent with our analysis of the flow of (4.20) above. Combining the obtained information about the flow on the two charts $y > 0$ and $z > 0$ given by (4.20) and (4.22) (those cover the segment of the blown-up circle that belongs to the first quadrant) we conclude that there is a hyperbolic sector at E_1 that belongs to the upper half-plane (see Figure 4.1, panels b) and a)).

Upon η crossing the value η_H, the equilibrium at B undergoes a subcritical Hopf bifurcation (see Figure 4.2 for illustration), thus generating a manifold of orbits that connect the unstable periodic orbit created by the Hopf bifurcation to the stable equilibrium at B which is a sink. In addition, there exists a heteroclinic orbit that asymptotically connects the saddle at A to an unstable periodic orbit around B. The proof of the Theorem 4.1 is completed.

Remark 4.3. *We note that it follows from the behavior of the vector field near infinity that when $0 < \alpha < \gamma < 1$ there exists a periodic orbit in (2.8) around the equilibrium B for any*

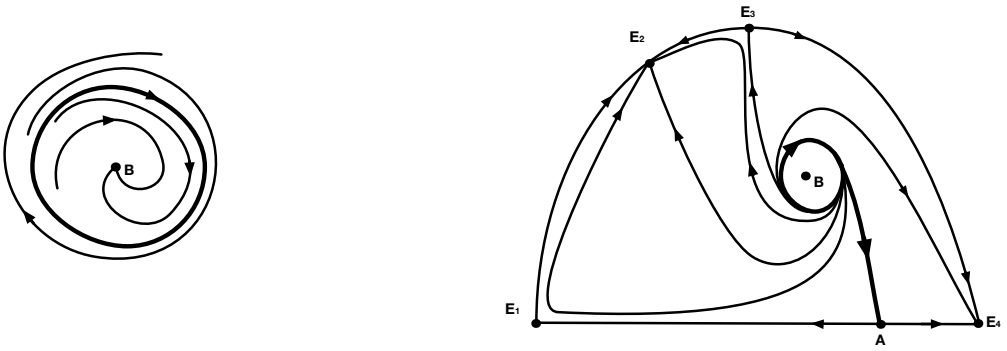

Figure 4.2. *An illustration for Theorem 4.1: A close-up picture for the dynamics near the equilibrium B and a heteroclininc orbit that connects a periodic orbit around the equilibrium B with the equilibrium A.*

$\eta < \eta_H$ since B is a stable node. This also implies the existence of heteroclinic orbits such as described in Theorem 4.1.

Acknowledgements. The authors would like to thank the anonymous referees for insightful feedback.

REFERENCES

[1] A. A. Andronov, E. A. Leontovich, I. I. Gordon, A. A. Maier, *Theory of Bifurcations of Dynamical Systems on a plane*, Israel Program for Scientific Translations, Jerusalem, 1971.
[2] C. Chicone, *Ordinary differential equations with applications*, Springer Texts in Applied Mathematics, 34, 2006.
[3] C. Chicone, J. Sotomayor, *On a Class of Complete Polynomial Vector Fields in the Plane.* J. Dif. Equations **61** (1986), 398-418.
[4] E. J. Doedel, R. C. Paffenroth, A. Champneys, T. F. Fairgrieve, Y. A. Kuznetsov, B. E. Oldman, B. Sandstede, X. Wang 2001 AUTO 2000: continuation and bifurcation software for ordinary differential equations (with Hom- Cont). Technical report, Concordia University (http://indy.cs.concordia.ca/auto/).
[5] G. F. D. Duff, *Limit-cycles and rotated vector fields*, Analysis of Mathematics, **57** (1953), 15-31.
[6] F. Dumortier, J. Llibre, J. C. Artés, *Qualitative Theory of Planar Differential Systems*, Springer, Berlin, 2006.
[7] N. Fenichel, *Geometric singular perturbation theory for ordinary differential equations*, J. Differential Eqs. **31** (1979), 53-98.
[8] P. C. Fife, *Asymptotic States for Equations of Reaction and Diffusion*, Bull. AMS **84** (1978), 693-726.
[9] C. K. R. T. Jones, *Geometric singular perturbation theory*, in Dynamical Systems (Montecatini Terme, 1994), Lecture Notes in Math. **1609**, Springer, Berlin, 1995, 44-118.
[10] Q. X. Liu, A. Doelman, V. Rottschäfer, M. de Jager, P. M. Herman, M. Rietkerk, J. van de Koppel, *Phase separation explains a new class of self-organized spatial patterns in ecological systems,* Proc Natl. Acad. Sci USA. **110** (2013), 11905-11910.
[11] Q. X. Liu, E. J. Weerman, P. M. Herman, H. Olff, J. van de Koppel, *Alternative mechanisms alter the emergent properties of self-organization in mussel beds,* Proc. Biol. Sci. **279** (2012), 2744-2753.
[12] L. M. Perko, *Rotated vector fields*, J. Diff. Eqns, **103** (1993), 127-145.

[13] L. M. Perko, *Differential Equations and Dynamical Systems*, second edition, Springer Texts in Applied Mathematics, 1998.

[14] J. van de Koppel, M. Rietkerk, N. Dankers, P. M. J. Herman, *Scale-dependent feedback and regular spatial patterns in young mussel beds.* Am. Nat. **165** (2005), E66-E77.

[15] R. -H. Wang, Q. -X. Liu, G. -Q. Sun, Z. Jin, J. van de Koppel. Nonlinear dynamic and pattern bifurcations in a model for spatial patterns in young mussel beds. J. R. Soc. Interface **6** (2009), 705-718.